

Group delay measurement of fiber Bragg grating resonances in transmission: Fourier transform interferometry versus Hilbert transform

Marie-Claude N. Dicaire,¹ Jeremy Upham,^{1,*} Israel De Leon,¹ Sebastian A. Schulz,¹ and Robert W. Boyd^{1,2,3}

¹*Department of Physics, University of Ottawa, Ottawa ON K1N 6N5, Canada*

²*The Institute of Optics, University of Rochester, Rochester, New York 14627, USA*

³*School of Physics and Astronomy, University of Glasgow, Glasgow, Scotland, UK*

*Corresponding author: jupham@uottawa.ca

Received January 29, 2014; revised March 10, 2014; accepted March 10, 2014;
posted March 12, 2014 (Doc. ID 205527); published April 8, 2014

Several methods exist to measure the group delay of a fiber Bragg grating. Here, we compare two such methods, namely the Hilbert transform (HT) of the device transmission spectrum and standard Fourier spectral interferometry. Numerical simulations demonstrate that both methods work not only for ideal, lossless devices but also for ones with realistic absorption. Experimental measurements show that the HT is more straightforward to implement and is significantly less susceptible to phase noise, which can significantly reduce the standard deviation between measurements. © 2014 Optical Society of America

OCIS codes: (060.3735) Fiber Bragg gratings; (120.5050) Phase measurement.

<http://dx.doi.org/10.1364/JOSAB.31.001006>

1. INTRODUCTION

The complete optical characterization of fiber Bragg gratings (FBGs) is necessary as a large variety of device designs are used for applications in diverse fields, ranging from dispersion compensators [1,2] and filters [3] in optical telecommunications, to temperature and strain sensors [4,5] throughout industry. This characterization comprises the amplitude response, which describes the transmission and reflection characteristics of the system, as well as the phase response, which describes its group delay. The group delay of a device is the time required for the amplitude envelope's peak to propagate along its length. This is most easily conceptualized as the time required for a pulse of light to travel through the system, but can also be applied to continuous wave inputs. Knowing the group delay of an FBG is very important, as it affects many phenomena, such as pulse propagation in signal processing and enhanced light-matter interactions in sensors and nonlinear optical components [6–8].

Several approaches for measuring the group delay of an FBG exist, and they can be split into two distinct categories: direct and indirect methods. Direct methods are time-domain based and include a measurement of the delay incurred by an optical pulse transmitted through the FBG [9,10]. However, these methods are generally limited by the time resolution of the measurement equipment and the challenge of matching the probe pulse and device bandwidths. The more commonly used indirect, frequency-domain-based methods extract the phase response of the device as a function of input frequency, $\phi(\omega)$, using mathematical transforms. This phase $\phi(\omega)$ is then used to calculate the group delay according to

$$\tau_g(\omega) = -\frac{d\phi(\omega)}{d\omega}. \quad (1)$$

A well-known example of such an indirect method is Fourier transform spectral interferometry (FTSI), where the phase information is extracted from an interferometric measurement [11,12]. Although functional, we will show in this work that it can be highly susceptible to phase noise, adding uncertainty to the final group delay values. Alternatively, we can use Hilbert transforms (HTs) [13,14] to extract the phase of an optical spectrum. However the HT can only be applied to causal functions. Furthermore, as we will discuss later, it can only be used to correctly extract the phase information if the input spectrum is phase minimum [15].

The reflection spectrum of a realistic FBG is generally not a minimum phase function, and so extra care and interferometric setups are necessary to meet this condition [16–18]. However, the transfer function of an FBG in transmission is always minimum phase, and therefore all necessary conditions are met [19]. Consequently, we are able to extract the phase information directly from a transmission spectrum, without the need for an interferometric setup, greatly simplifying experimental procedures. Previous numerical work has shown that the HT method works for the case of lossless FBGs [19]. Furthermore, experimental work has shown that it works for photonic crystals in the radio frequency regime [20].

In this work, we compare the HT and FTSI methods for measuring group delays in realistic FBGs in a transmission geometry. First, we present a summary of the underlying mathematical analysis, showing how both methods extract the phase information from their respective optical measurements, followed by a discussion of their similarities and differences. In the final sections, we compare the accuracy of the HT and FTSI methods, both numerically and experimentally. For these comparisons, we use a rectified Gaussian FBG, which consists of a constant Bragg period with a Gaussian

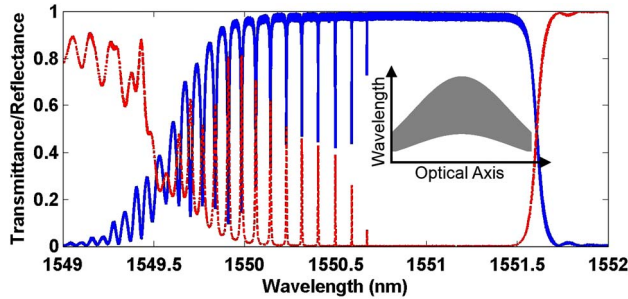


Fig. 1. Experimental transmittance (dashed red) and reflectance (solid blue) curves of a rectified Gaussian FBG. The narrow peaks are the result of a resonant cavity inside the photonic bandgap. Inset: bandgap diagram of the same device along the fiber axis. The shaded area represents the bandgap, where propagation of light is forbidden. At short wavelengths, the propagating region is bounded by two forbidden regions, thus creating a cavity where light resonates.

distribution of the refractive index modulation along the optical axis [21,22], which results in narrow bandwidth resonances with a large range of group delays. The photonic bandgap widens as the index modulation gets larger, and the center wavelength of the local bandgap shifts in response to the local mean refractive index change (inset of Fig. 1). The aforementioned narrow bandwidth resonant modes are confined between spatial bandgap regions on the short wavelength side of the bandgap. The measured transmittance and reflectance spectra, taken with a narrow linewidth continuous wave source swept through the spectral region of interest with 0.1 pm resolution, of such a Gaussian FBG are shown in Fig. 1, where some of the resonant peaks have bandwidths narrower than 1 pm. Rectified Gaussian FBGs have the potential to be used as sophisticated sensors due to the resonant features' large group delays and narrow bandwidths [5] or devices capable of significant nonlinear optical responses due to the large field intensity enhancements in the resonant modes [23]. However, the challenge of accurately measuring large group delay values at a sufficiently fine spectral resolution is significant.

2. THEORY

As they are indirect group delay measurements, both the HT and FTSI methods extract the phase information from a frequency-based input. The input for the HT is a simple transmission spectrum, while FTSI needs an interference spectrum. In both cases the group delay $\tau_g(\omega)$ is then found using Eq. (1).

A. Hilbert Transform

The HT, \mathcal{H} , can be used to relate the imaginary and real parts of a linear function $G(\omega)$, provided it is causal in the time domain; i.e., $g(t) = 0$ for $t < 0$, where $g(t)$ is the inverse Fourier transform of $G(\omega)$. The HT is given by

$$\mathcal{H}[\Im[G(\omega_0)]] = \frac{1}{\pi} \int_{-\infty}^{+\infty} \frac{\Re[G(\omega)]}{\omega - \omega_0} d\omega = \Re[G(\omega_0)], \quad (2)$$

where $\Im[G(\omega)]$ and $\Re[G(\omega)]$ are the imaginary and real parts of the linear function $G(\omega)$, respectively, and we evaluate the Cauchy principal value of the integral to account for the pole at $\omega = \omega_0$. The inverse HT is defined as $\mathcal{H}^{-1} = -\mathcal{H}$. Familiar examples of a HT are the Kramers–Kronig relations, which are

valid only if $G(\omega)$ is Hermitian, i.e., the real part is even while the imaginary part is odd. For the purpose of this work we use the more general HT as defined above.

Upon inspection of Eq. (2) we note that the integral is the convolution of $\Im[G(\omega)]$ and $1/\pi\omega$. Hence we can write an equivalent definition of the HT using Fourier transforms

$$\mathcal{H}[\Im[G(\omega)]] = -\mathcal{F}^{-1}[i \operatorname{sgn}(t) \cdot \mathcal{F}[\Im[G(\omega)]]], \quad (3)$$

where $\operatorname{sgn}(t)$, \mathcal{F} , and \mathcal{F}^{-1} are the signum function, Fourier transform, and inverse Fourier transform, respectively. This definition is better suited for numerical implementations as it removes the pole present in Eq. (2). Furthermore, we can make use of fast Fourier transforms, which significantly reduces computation time.

As clearly shown in the definition of the HT [Eq. (2)], it links the real and imaginary parts of a function. Therefore, in order to extract the phase information of an optical system using the HT, it is necessary to find a function that separates the amplitude and phase information into its real and imaginary parts. We recall that the transmission coefficient $t(\omega)$ of an optical system is defined as

$$t(\omega) = \sqrt{T(\omega)} e^{i\phi(\omega)}, \quad (4)$$

where $T(\omega)$ is the transmittance. We invoke the natural logarithm to separate the real and imaginary parts of $t(\omega)$:

$$\ln t(\omega) = \frac{\ln T(\omega)}{2} + i\phi(\omega). \quad (5)$$

We can now apply the HT to $\ln(T(\omega))$, yielding the phase $\phi(\omega)$. As stated earlier, the HT can only be applied if the function is causal, and therefore we require $\ln(T(\omega))$ to be causal. This is the case if $t(\omega)$ is a minimum phase function [15], conditions that are always satisfied by the transmission through a FBG [19].

One further modification to the HT is necessary in order to implement this method experimentally. The integral in Eq. (2) ranges from $-\infty$ to ∞ ; however, we cannot practically know $T(\omega)$ for all frequencies. We therefore approximate the HT by covering a sufficient bandwidth. The chosen bandwidth can be considered sufficient if the start and end points are far enough away from any optical bandgap, such that the optical delay at these points is locally frequency independent and can be approximated as the delay incurred while traveling through a piece of fiber with a length equal to the FBG. The final relation between the phase and amplitude information can therefore be expressed as

$$\phi(\omega_0) = -\frac{1}{2\pi} \int_{\omega_1}^{\omega_2} \frac{\ln[T(\omega)]}{\omega - \omega_0} d\omega - \omega_1 \tau_1, \quad (6)$$

where ω_1 and ω_2 correspond to the start and end frequencies of the spectrum shown in Fig. 1 and τ_1 corresponds to the delay incurred at ω_1 .

B. Fourier Transform Spectral Interferometry

As the name suggests, the FTSI method is an analysis method for interferometric data [11]. In this discussion we will use the example of a Mach–Zehnder interferometer, as shown in

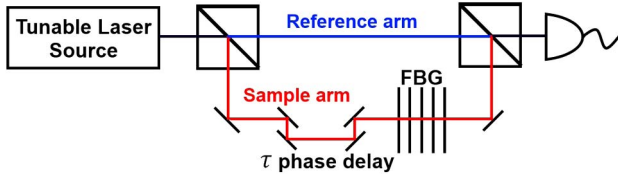


Fig. 2. Sketch of a Mach-Zehnder interferometer, suitable for the FTSI method. The optical input is split into two arms, one short reference arm and a longer arm containing the sample under investigation, where τ_F is the time delay associated with the total length difference between the two arms at frequencies far from the bandgap.

Fig. 2, although the method can be applied to other interferometer designs. It is important to notice that for a simplified analysis the reference arm should be slightly shorter than the sample arm, where the time delay associated with the total length difference between the two arms at frequencies far from the bandgap is described by τ_F .

Upon recombination, the light from the two arms interferes, resulting in the intensity spectrum

$$I(\omega) = S(\omega) + R(\omega) + 2\sqrt{S(\omega)R(\omega)} \cos(\phi(\omega) - \omega\tau_F). \quad (7)$$

Here $S(\omega)$ and $R(\omega)$ are the sample and reference arm transmittances, respectively, $\omega\tau_F$ is the phase delay due to the difference in optical arm length, and $\phi(\omega)$ is the sample induced phase difference. The interference term of Eq. (7) (the third term) can be isolated by either measuring it directly using a balanced photodetector or measuring $S(\omega)$ and $R(\omega)$ separately and then subtracting them from $I(\omega)$. We take the Fourier transform of this isolated interference signal and get three peaks: a DC component at $t = 0$ and two at $t = \pm\tau_F$, characterizing the interference term. We then isolate one of the interference peaks at $t = \pm\tau_F$ with a window function and take the inverse Fourier transform. This results in the phase term according to

$$\phi(\omega) = \arg[\mathcal{F}^{-1}(W(t) \cdot \mathcal{F}(I(\omega)))] + \omega\tau_F, \quad (8)$$

where $W(t)$ is a window function over one of the interference peaks at $t = \pm\tau_F$.

C. Similarities and Differences

Both methods extract the phase information, and Eq. (1) is then used to obtain the group delay, resulting in two very similar mathematical forms: for the FTSI method,

$$\tau_g(\omega) = -\frac{d}{d\omega} \{ \arg[\mathcal{F}^{-1}(W(t) \cdot \mathcal{F}(I(\omega)))] \} - \tau_F + \tau_1, \quad (9)$$

and for the HT method,

$$\tau_g(\omega) = -\frac{d}{d\omega} \left\{ \mathcal{F}^{-1} \left(i \operatorname{sgn}(t) \cdot \mathcal{F} \left(\frac{\ln(T(\omega))}{2} \right) \right) \right\} + \tau_1, \quad (10)$$

where $T(\omega)$ from the HT is equivalent to $S(\omega)$ from the FTSI analysis above. However, while there are mathematical similarities between these two methods, there are significant differences that need to be considered. Mathematically, the FTSI is a method to extract part of a function, while the HT relates different parts of a function to each other. Consequently, the HT needs an additional condition, causality,

which in our case translates to the minimum phase condition for $t(\omega)$. However, as stated before, these conditions are always met for the transmission spectrum of a FBG. The major difference between the two methods lies in the experimental implementations necessary to collect the input spectra. The FTSI method requires an interference setup, while the HT can use a simple transmission spectrum. In the next sections we will investigate the effect of this difference on the accuracy of the two methods.

3. NUMERICAL RESULTS

Here we compare the accuracy of the two methods numerically, representing the case of an “ideal”, i.e., noise-free, experiment. To do this, we simulate the propagation of light through a rectified Gaussian FBG over the wavelength range of interest using a transfer matrix method, yielding its transmission and phase spectra. By applying Eq. (1) to this phase, we find the true value of the group delay. We then use the transmission spectrum to get the HT derived group delay, and an interference spectrum (created by numerically interfering the transmission with a reference signal) to get the FTSI derived group delay. Therefore we end up with three group delay spectra: one true spectrum and one for each of the different measurement methods. Figure 3 compares both methods to the true group delay values for a lossless device. The transmission peaks narrow in bandwidth as they penetrate deeper in the bandgap (shown in Fig. 1). Consequently, these resonant modes will have proportionally larger group delays [5]. The group delay peaks are accurately recovered by both methods, within the limitation of resolution of the peaks. The discrepancy of the curves in the gaps between the resonant peaks can be described as follows: the transfer matrix method can output accurate phase information even when transmitting negligible power, thus producing constant values between the peaks. Conversely, the FTSI and HT methods, which depend on nonzero amplitude information, contend with numerical noise from the simulations’ approximation of zero. Therefore, both methods can be set to accurately determine group delay provided some transmission signal exists. Figure 4 repeats the simulation with linear absorption losses uniformly applied along the length of the FBG in order to approximate the losses incurred in realistic devices [23,24]. While losses reduces the group delay value of each peak, both methods continue to accurately measure these values.

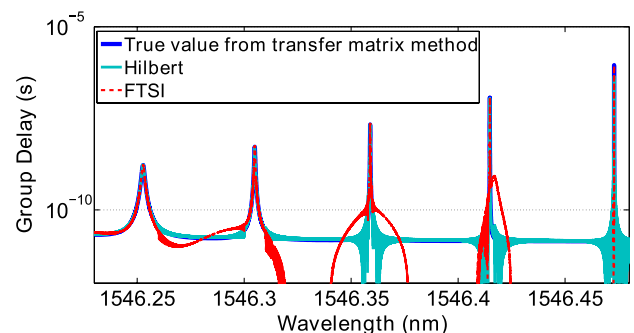


Fig. 3. Numerical group delay spectra for a lossless rectified Gaussian FBG. The different lines are hard to distinguish as the HT and FTSI derived group delays agree well with the actual group delay.

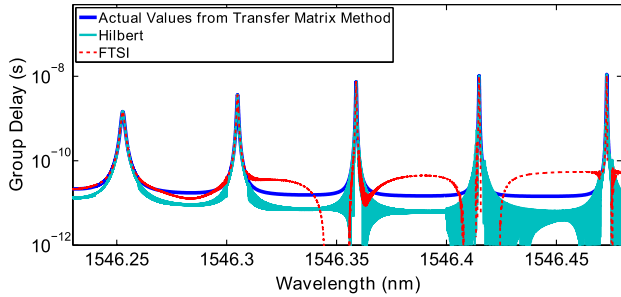


Fig. 4. Same case as Fig. 3, in the presence of absorption losses. Even with loss, both the HT and FTSI derived group delays still agree well with the true value.

4. EXPERIMENTAL RESULTS

For the experimental comparison, we measured the transmission and interference spectra of the rectified Gaussian FBG and used both the FTSI and HT methods to derive the group delay spectra. As with the transmission and reflection spectra in Fig. 1, all measurements were done with a 100 kHz linewidth tunable continuous wave laser that was swept over the spectrum of interest at 0.1 pm resolution. For the transmission spectrum, the transmitted light is measured using a photodiode. For the interference measurement, we place the FBG inside a Mach–Zehnder interferometer, as shown in Fig. 2, and use a balanced photodiode to isolate the interference signal. These measurements are repeated several times (20 times for the transmittance and 18 times for the interference), allowing us to calculate the uncertainty associated with each method. The resulting group delay spectra are shown in Fig. 5 (red curve represents HT data, and blue represents FTSI). There are two striking observations to be made. First of all, the HT method shows significant noise between the group delay peaks. In this region, very little or no light is transmitted and therefore the only signal within the transmission spectrum is noise, such as dark currents in the detector, while in the interferometric measurement we still have a significant signal due to the reference arm. However, as no light is transmitted through the FBG in this region, the delay at these wavelengths is of no interest. Instead, we should examine the spectra around the delay peaks, as shown in the insets of Fig. 5. Here the HT method has a significantly lower uncertainty (solid color area) than the FTSI method, while the mean delay of the two measurement (thin lines) approaches in good agreement. The higher uncertainties of the FTSI data are attributed to the interference measurement accumulating phase noise between the two arms of the interferometer from a variety of factors, such as temperature variations and external vibrations. Because the HT requires only the transmission intensity, it is insensitive to fluctuation in phase.

Since the absolute value of the standard deviation increases with the group delay of a resonance mode, we normalize it to the mean group delay value measured for each peak in order to quantify the uncertainty associated with each method. The reduced uncertainty of the HT method is clearly apparent in Fig. 6, which shows the standard deviation of each peak normalized to the peak height. For the FTSI method, the uncertainty lies in the range of 25%–185%, while the corresponding values for the HT method do not exceed 10%.

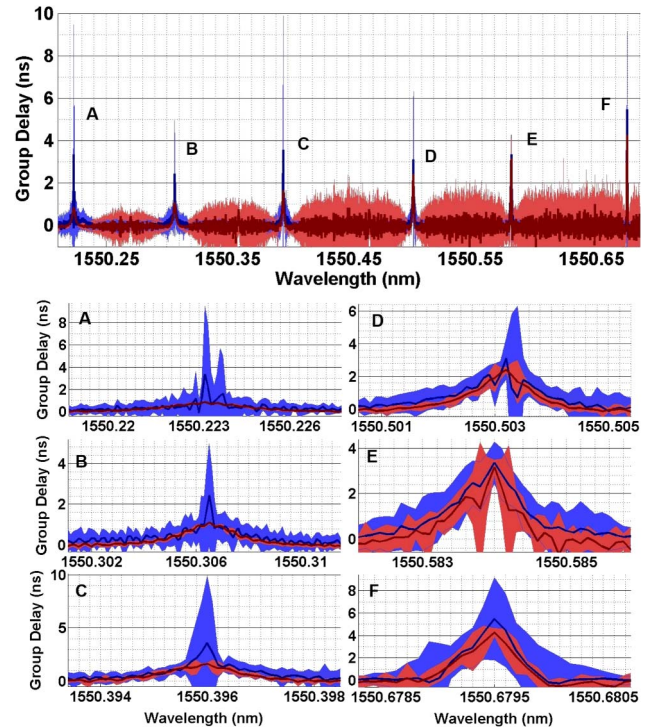


Fig. 5. Group delay spectra obtained experimentally with FTSI (blue) and HT (red) methods. The lines represent the average group delay values, while the shaded regions represent the associated standard deviation. Top: overview of the whole region of interest. The HT method has a large uncertainty between the peaks, as there is no transmission: only random noise, with random phase, is detected. The FTSI method has less noise in that region because there is still transmission from the reference arm. However, this is not a concern since we are only interested in the peak values. Bottom images: zoomed-in spectra of the group delay peaks. The average values are in good agreement, and the standard deviation for the HT method is consistently lower than the FTSI standard deviation, indicating a cleaner measurement.

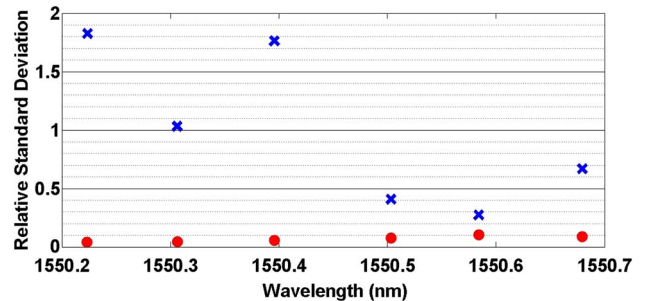


Fig. 6. Standard deviation of the group delay peaks, normalized to the peak height. The FTSI method (blue crosses) has large uncertainties, ranging from 25% to 185%. The HT method's (red dots) uncertainties are much better, at most 10% of the peak height.

5. CONCLUSION

Using numerical simulations, we showed that both the FTSI and HT methods are capable of extracting the group delay of narrow resonance peaks in a realistic FBG (including absorption losses) with equal accuracy. However, an experimental comparison shows that their susceptibility to sources of noise is quite different. The interferometric approach is more susceptible to phase noise being introduced into the

sample or reference arms by the environment, such as vibrations or temperature fluctuations. Because the HT method measures only the transmission data of the device, it is not affected by phase variations in the signal. Furthermore, with this method a single measurement using a single source and detector allows full characterization of the amplitude and phase response of an FBG. Conversely, the FTSI method requires an interferometric setup and either a more complicated detection setup (balanced photodiodes) or multiple measurements (one for each arm separately and then the interference signal) to isolate the sample response. In our comparative experiments using the same instrumentation, the HT method led to a much smaller uncertainty (<10%) compared to the FTSI method (between 25% and 185%). Both methods can still be affected by intensity noise (source fluctuation or detector dark currents), and the magnitude of the impact of noise on measurements will depend on instrumentation and environment, but removing phase noise as a source of error is a compelling reason to use the HT approach for group delay characterization of FBGs. While the HT method can only be used under certain conditions (a causal $\ln[t(\omega)]$, which can be ensured by a minimum phase $t(\omega)$), these conditions are always fulfilled for the transmission through a FBG. Therefore, we have shown that the HT is not only a valid method for measuring group delays, but also offers significant advantages in both accuracy and ease of measurement when compared to the FTSI method.

ACKNOWLEDGMENTS

The research was supported by the Canada Excellence Research Chairs (CERC) program.

REFERENCES

1. F. Ouellette, "Dispersion cancellation using linearly chirped Bragg grating filters in optical waveguides," *Opt. Lett.* **12**, 847–849 (1987).
2. N. M. Litchinitser, B. J. Eggleton, and D. B. Patterson, "Fiber Bragg gratings for dispersion compensation in transmission: theoretical model and design criteria for nearly ideal pulse recompression," *J. Lightwave Technol.* **15**, 1303–1313 (1997).
3. A. M. Vengsarkar, P. J. Lemaire, J. B. Judkins, V. Bhatia, T. Erdogan, and J. E. Sipe, "Long-period fiber gratings as band-rejection filters," *J. Lightwave Technol.* **14**, 58–65 (1996).
4. A. D. Kersey, M. A. Davis, H. J. Patrick, M. LeBlanc, K. P. Koo, C. G. Askins, M. A. Putnam, and E. J. Friebele, "Fiber grating sensors," *J. Lightwave Technol.* **15**, 1442–1463 (1997).
5. H. Wen, M. Terrel, S. Fan, and M. Dignonnet, "Sensing with slow light in fiber Bragg gratings," *IEEE Sens. J.* **12**, 156–163 (2012).
6. B. J. Eggleton, R. E. Slusher, C. M. de Sterke, P. A. Krug, and J. E. Sipe, "Bragg grating solitons," *Phys. Rev. Lett.* **76**, 1627–1630 (1996).
7. A. Melloni, M. Chinello, and M. Martinelli, "All-optical switching in phase-shifted fiber Bragg grating," *IEEE Photon. Technol. Lett.* **12**, 42–44 (2000).
8. R. W. Boyd, "Material slow light and structural slow light: similarities and differences for nonlinear optics," *J. Opt. Soc. Am. B* **28**, A38–A44 (2011).
9. J. T. Mok, M. Ibsen, C. M. de Sterke, and B. J. Eggleton, "Dispersionless slow light with 5-pulse-width delay in fibre Bragg grating," *Electron. Lett.* **43**, 1418–1419 (2007).
10. H. Shaoei, M. Li, and J. Yao, "Continuously tunable time delay using an optically pumped linear chirped fiber Bragg grating," *J. Lightwave Technol.* **29**, 1465–1472 (2011).
11. A. Gomez-Iglesias, D. O'Brien, L. O'Faolain, A. Miller, and T. Krauss, "Direct measurement of the group index of photonic crystal waveguides via Fourier transform spectral interferometry," *Appl. Phys. Lett.* **90**, 261107 (2007).
12. C. Dorrer, N. Belabas, J.-P. Likhforman, and M. Joffe, "Spectral resolution and sampling issues in Fourier-transform spectral interferometry," *J. Opt. Soc. Am. B* **17**, 1795–1802 (2000).
13. K.-E. Peiponen and E. M. Vartiainen, "Kramers-Kronig relations in optical data inversion," *Phys. Rev. B* **44**, 8301–8303 (1991).
14. B. E. A. Saleh and M. C. Teich, *Fundamentals of Photonics*, 2nd ed. (Wiley, 2007).
15. A. Papoulis, *The Fourier Integral and Its Applications* (McGraw-Hill, 1962).
16. A. Carballar and C. Janer, "Complete fiber Bragg grating characterization using an alternative method based on spectral interferometry and minimum-phase reconstruction algorithms," *J. Lightwave Technol.* **30**, 2574–2582 (2012).
17. A. Mecozzi, "Retrieving the full optical response from amplitude data by Hilbert transform," *Opt. Commun.* **282**, 4183–4187 (2009).
18. R. H. J. Kop, P. de Vries, R. Sprik, and A. Lagendijk, "Kramers-Kronig relations for an interferometer," *Opt. Commun.* **138**, 118–126 (1997).
19. L. Poladian, "Group-delay reconstruction for fiber Bragg gratings in reflection and transmission," *Opt. Lett.* **22**, 1571–1573 (1997).
20. M. J. Erro, I. Arnedo, M. A. G. Laso, T. Lopetegi, and M. A. Muriel, "Phase-reconstruction in photonic crystals from S-parameter magnitude in microstrip technology," *Opt. Quantum Electron.* **39**, 321–331 (2007).
21. J. E. Sipe, L. Poladian, and C. M. de Sterke, "Propagation through nonuniform grating structures," *J. Opt. Soc. Am. A* **11**, 1307–1320 (1994).
22. T. Erdogan, "Fiber grating spectra," *J. Lightwave Technol.* **15**, 1277–1294 (1997).
23. J. Upham, I. De Leon, D. Grobncic, E. Ma, M.-C. N. Dicaire, S. A. Schulz, S. Murugkar, and R. W. Boyd, "Enhancing optical field intensities in Gaussian-profile fiber Bragg gratings," *Opt. Lett.* **39**, 849–852 (2014).
24. I. C. M. Littler, T. Grujic, and B. J. Eggleton, "Photothermal effects in fiber Bragg gratings," *Appl. Opt.* **45**, 4679–4685 (2006).